Topological analysis of the electron localization function applied to delocalized bonds

A. Savin, B. Silvi, and F. Colonna

Abstract: What is a local viewpoint of delocalized bonds? We try to provide an answer to this paradoxical question by investigating representative conjugated organic molecules (namely, allyl cation, *trans*-butadiene, and benzene) together with reference nonconjugated systems (ethylene and propene) by means of topological analysis of the electron localization function ELF. The valence attractors of the ELF gradient field are classified according to their synaptic order (i.e., connections with core attractors). The basin populations $\bar{N}$, (i.e., the integrated density over the attractor basins) and their standard deviation, σ, have been calculated and are discussed. The basin populations and their relative fluctuations, defined as $\lambda = \sigma^2/\bar{N}$, are sensitive criteria of delocalization. In the case of well-localized C—C or C=C bonds, $\lambda \sim 0.4$, whereas for delocalized bonds λ increases to about 0.5. Another criterion of delocalization is provided by the basin hierarchy, which is defined from the reduction of the localization domains. For most systems, delocalization occurs not only for neighboring carbon–carbon disynaptic attractor basins, but also for nearest neighbor disynaptic protonated attractor basins.

Key words: electron localization function, topological analysis, delocalization, population analysis.

Résumé : Y a-t-il un point de vue local des liaisons délocalisées ? Nous essayons de répondre à cette question pour le moins paradoxale en examinant une série de molécules organiques conjuguées et de systèmes non-conjugués de référence à l'aide de l'analyse topologique de la fonction de localisation ELF. Ces systèmes sont d'une part le cation allyl, le *trans*-butadiène et le benzène et, d'autre part l'éthylène et le propène. Les attracteurs de valence du champ gradient de ELF sont classés suivant leur order synaptique (c'est à dire, suivant le nombre de connections qu'ils forment avec les cœurs). La population moyenne par bassin, $\bar{N}$, et son écart-type, σ, ont été calculés et font l'objet d'une discussion. Les populations moyennes par bassin et leurs fluctuations relatives, $\lambda = \sigma^2/\bar{N}$, sont des indicateurs sensibles de la délocalisation. Pour des liaisons C—C ou C=C localisées, $\lambda \sim 0.4$ tandis que pour des liaisons plus délocalisées $\lambda \sim 0.5$. La hiérarchie des bassins, définie à partir de la réduction des domaines de localizations, est un autre critère de délocalisation. Dans la plupart des systèmes la délocalisation affecte non seulement les bassins des attracteurs relatifs au squelette carboné mais également les bassins adjacents d'attracteurs disynaptiques protonés.

Mots clés : fonction de localisation d'électrons, analyse topologique, délocalisation, analyse de population.

1. Introduction

The bonding in conjugated organic systems cannot be represented by a definite Lewis structure and is therefore referred as delocalized. Attempts at understanding such systems on the basis of the Lewis theory of valence have given rise to, for example, chimerical structures such as those proposed by Huggins (1), which were rejected with the advent of quantum chemistry. The valence-bond (VB) and molecular orbital (MO) approaches are at the root of the two basic descriptions of these bonds that can be found in textbooks (2). On the one hand is the resonance concept, in which the true ground state wave function of the system is expressed as a linear combination of wave functions corresponding to definite Lewis structures (3), and on the other hand is the MO description in which the bonding orbitals are delocalized over the whole molecule. As mentioned by Coulson (4): "There is an interesting contrast between the VB and MO descriptions of benzene. Both require complete delocalization, but whereas the VB method introduces it by superposition of Kekulé (and other) structures, in the MO method there is nothing that even remotely resembles a structure. This situation warns us once more against any too literal belief in the reality of our structures." This epistemological difficulty is mostly due to the weakness of interpretative methods that give a physical significance to quantities, such as molecular orbitals or valence-bond structures, appearing as intermediate during the course of approximate procedures of solution of the many-body Schrödinger equation.

The analysis of local functions defined within the exact many-body theory, such as the electron densities and deformation densities, is an alternative interpretative strategy that is more consistent with the interpretative postulates of quantum mechanics. The difficulty is then to find a guideline

Received November 1, 1995.

This paper is dedicated to Professor Richard F.W. Bader on the occasion of his 65th birthday.

A. Savin, B. Silvi,[1] and F. Colonna. Laboratoire de chimie théorique (URP 9070), Université Pierre et Marie Curie, 4, Place Jussieu, 75252 Paris cédex 05, France.

[1] Author to whom correspondence may be addressed. Telephone: +31-1-4427-4053. Fax: +31-1-4427-4117. E-mail: silvi@lct.jussieu.fr

allowing an objective partition of the molecular space and to make a link with the ideas widespread in the chemistry community. With respect to the delocalization problem, the question of the description provided by such local theories may seem to be paradoxical. In an early version of the loge theory, delocalization in benzene could be accounted for by the presence of "one loge with six delocalized electrons and extending over the carbon cores" (5). This assumption has not been supported by calculations since the numerical complexity of the determination of the boundaries of such a loge is too high to be feasible. The theory of atoms in molecules (6) provides a partition of the molecular space into atomic basins. Though these basins cannot by themselves provide a picture of the delocalization, the definition of bond orders within this framework (7, 8) provides a proper framework for the discussion of the delocalization.

An alternative partition of the molecular space is provided by topological analysis of the electron localization function ELF (9), which yields basins related to the local pairing of electrons. In this paper, we have investigated by this technique the bonding in simple hydrocarbons containing double and single bonds (namely ethylene, propene, allyl cation, *trans*-butadiene, and benzene) in order to compare the local properties in typical localized and delocalized systems.

2. A sketch of the topological analysis of the ELF function

The topological analysis of molecular space has been pioneered for two decades by Richard Bader (6) who investigated the gradient field of the electron density in order to build a rigorous theory of the chemical bond. Gradient field analysis is the mathematically well-established method allowing "access to a rigorous qualitative thinking" (10). In the particular field of the chemical bond, it can help to objectively define the words used to describe molecules on a microscopic scale. In this respect, Bader's definition of the atom within the molecule exemplifies the possibilities of the method. In principle, gradient field analysis can be applied to any well-defined local function. For us, a well-defined local function is a function of the space coordinate $\boldsymbol{r}$, which can be expressed in the framework of an exact many-body theory. Property densities are defined as the integral over the spin coordinate:

$$[1] \qquad \rho_A(\boldsymbol{r}) = \int \hat{A}\rho(\boldsymbol{x};\boldsymbol{x}')_{\boldsymbol{x}'=\boldsymbol{x}}\mathrm{d}\sigma$$

$\hat{A}$ is the Hermitian operator associated with the property, $\rho(\boldsymbol{x},\boldsymbol{x}')$ is the first-order density matrix (11), and $\boldsymbol{x}$ stands for the space and spin coordinates. They are well-defined local functions whereas orbitals, in many-electron systems, have no physical meaning since they appear as mathematical intermediates during the calculation. Functions of densities of property are also local functions. As examples of well-defined local functions we can mention the electron density and derived quantities such as the molecular electrostatic potential. We have recently shown (9) that a similar analysis applied to a localization function such as that of Becke and Edgecombe (12) provides "a clear demarcation between shared-electron interaction, as in covalent and metallic bonding, and unshared-electron interactions, such as in ionic and hydrogen bonded systems" (13).

2.1. The physical significance of ELF

The ELF function proposed by Becke and Edgecombe (12) was originally defined within the framework of Hartree–Fock (approximate) theory as:

$$[2] \qquad \eta(\boldsymbol{r}) = \frac{1}{1+\left(\frac{D_\sigma}{D_\sigma^0}\right)^2}$$

in which D_σ and D_σ^0 represent the curvature of the electron pair density for electrons of identical σ spins (the Fermi hole) for, respectively, the actual system and a homogeneous electron gas with the same density. D_σ is the Laplacian of the conditional probability calculated from a single determinental Hartree–Fock wave function:

$$[3] \qquad D_\sigma = (\nabla_2^2 P_{\mathrm{cond}}^{\sigma\sigma}(1,2))_{1=2} = \sum_{i=1}^{N} |\nabla\varphi_i|^2 - \frac{1}{4}\frac{|\nabla\rho^\sigma(1)|^2}{\rho^\sigma(1)}$$

As mentioned before (14) this expression is formally identical to the difference between the positive definite local kinetic energy of a system of noninteracting fermions $T_s^\sigma[\rho]$ appearing in the Kohn–Sham equations (15) and that appearing in the von Weizsäcker functional (16).

$$[4] \qquad D_\sigma = T_s^\sigma[\rho] - \frac{1}{4}\frac{|\nabla\rho^\sigma(1)|^2}{\rho^\sigma(1)}$$

As pointed out by Tal and Bader (17), the von Weizsäcker functional (16) is a lower bound to the positive definite local kinetic energy that is locally approached at the Hartree–Fock level when a single orbital makes the dominant contribution to the density in the same region of space. The von Weizsäcker functional is also the positive definite local kinetic energy of a system of noninteracting particles of density ρ^σ for which the Pauli repulsion has been switched off. Therefore, D_σ signifies the local excess of kinetic energy due to the Pauli repulsion. The kinetic interpretation of D_σ (14) is very important because it extends the validity of the ELF function to the ground state of real systems for which $T_s^\sigma[\rho]$ can be exactly evaluated within density functional theory. Therefore, for ground state systems ELF gains the status of a well-defined local function. Furthermore, this definition of ELF allows its determination from knowledge of the electron density alone. Thus, instead of considering the Laplacian of the conditional probability, it is more advantageous to consider D_σ in its kinetic interpretation to redefine ELF. For closed-shell systems, $T_s^\alpha[\rho] = T_s^\beta[\rho] = \frac{1}{2}T_s[\rho]$ and $\rho^\alpha(\boldsymbol{r}) = \rho^\beta(\boldsymbol{r}) = \frac{1}{2}\rho(\boldsymbol{r})$, so:

$$[5] \qquad \begin{aligned} D_\sigma &= \frac{1}{2}T_s[\rho] - \frac{1}{8}\frac{|\nabla\rho(1)|^2}{\rho(1)} \\ D_\sigma^0 &= \frac{3}{10}(3\pi^2)^{2/3}\rho^{5/3}(1) \end{aligned}$$

In these expressions, the σ dependence no longer appears on

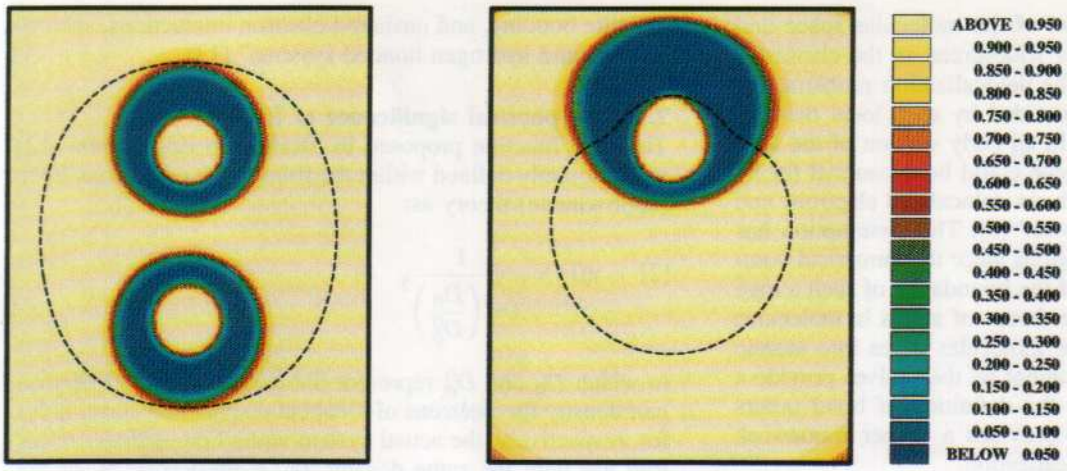

Fig. 1

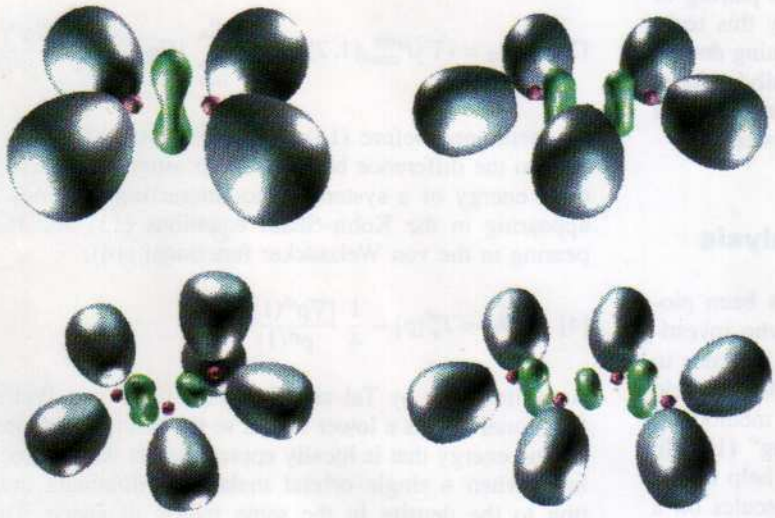

Fig. 2

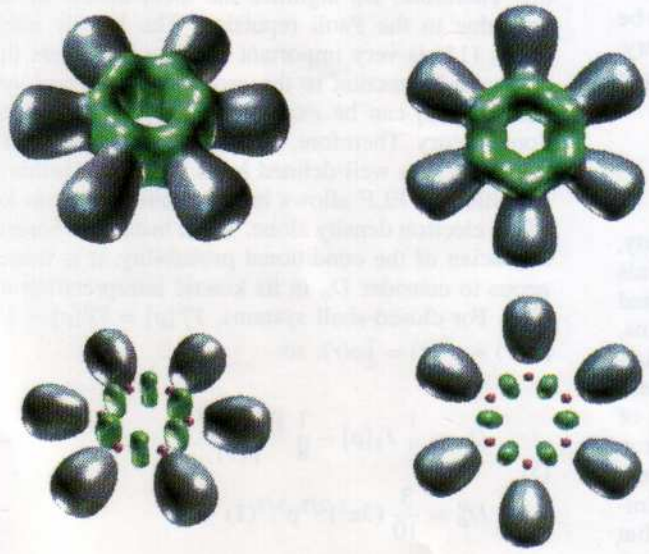

Fig. 3

Plate 1. Fig. 1. Representation of ELF for Li_2 (left) and LiH (right). ELF has been calculated with the density threshold ε set to zero. The value of ELF is given by the color scale. The broken lines correspond to the 10^{-3} e^- bohr^{-3} isodensity contours. **Fig. 2.** $\eta(\boldsymbol{r}) = 0.8$ localization domains of ethylene (top left), propene (bottom left), allyl cation (top right), and *trans*-butadiene (bottom right). The nature of the attractor defining the domain is given by the color code. Magenta: core; green: valence disynaptic; blue: protonated valence disynaptic. **Fig. 3.** The $\eta(\boldsymbol{r}) = 0.5$ and $\eta(\boldsymbol{r}) = 0.8$ localization domains of benzene. Same color code as in Fig. 2.

the right-hand side of the equations and therefore, one may consider D and D^0.[2]

In regions of space where the electron density is very low, the numerical representation of the wave function and of the density is not accurate enough to warrant the reliability of the gradients of local functions. Spurious attractors may appear that are due to computational artefacts such as roundoff errors or to basis set effects. Such troubles arise when D_σ tends to zero faster than $\rho(\boldsymbol{r})$. In practice, one can remove these difficulties by taking an effective ELF written as:

$$[6] \qquad \frac{1}{1+\left(\frac{D+\varepsilon}{D^0}\right)^2}$$

ε is chosen such that ELF tends to zero with the density ρ. In actual calculation we use $\varepsilon = 2.87 \times 10^{-5}$. This value constrains ELF to be less than 0.5 for $\rho \leq 10^{-3}$.

ELF is a local measure of the effect of the Pauli repulsion on the kinetic energy density. In the region of space where the Pauli repulsion is weaker than in a uniform electron gas of identical density (we should say, where the local parallel pairing is lower), ELF is close to 1 whereas where the local parallel pairing is higher (and therefore the Pauli repulsion strongly active) ELF is low. For example, in a closed-shell system, though the α and β spin densities are equal everywhere, there are regions of low ELF between high ELF regions.

2.2. The topological analysis of ELF

As ELF is a scalar function, the analysis of its gradient field allows us to locate attractors to which we have given a chemical signification (9). Usually, the attractors of a gradient field[3] are single points as is the case for the gradient field of the density. However, for the ELF function, they can also be circles and spheres if the system belongs to a continuous symmetry group (here, cylindrical and spherical symmetry, respectively). In actual cases, the local symmetry remains very strong and, effectively, circular and spherical attractors can be found in molecules belonging to finite symmetry groups. There are, basically, two types of attractors: core and valence attractors. The attractors are designated according to the presence of a nucleus (except a proton) within their basin. They are either points (K-shell attractors) or spheres for the outer core shells.

To offer an efficient visualization tool, we introduced f-localization domains (9), which we defined as formal bodies bounded by a given isosurface $\eta(\boldsymbol{r}) = f$ and enclosing points for which ELF $> f$. These localization domains[4] are the ELF analogs of Mezey's density domains (18). They are said to be reducible when they contain more than one attractor, irreducible when they contain one attractor. The graphical representation of the irreducible localization domains with color codes associated with the type of attractor provides explanatory pictures of the bonding in molecules and crystals.

A valence attractor is connected to a core attractor when the two following conditions are fulfilled.

(*i*) Their basins are bounded by a part of a common separatrix.

(*ii*) The valence attractor lies within the smallest (reducible or irreducible) valence f-localization domain that totally surrounds the core attractor basin in a chemically relevant region (i.e., within which the electron density is larger than 10^{-3} au (19)).

In principle, a core is always totally encapsulated by at least one valence basin and therefore propositions (*i*) and (*ii*) are redundant when f tends to zero unless the valence localization domains have already merged with a core domain. Figure 1 (see Plate 1) provides an example of the determination of

[2] A possible generalization of ELF, which is valid to any stationary state and which preserves the requirements of a well-defined local function, can be achieved by substituting $T_s[\rho]$ by the positive definite local kinetic energy density $G(\boldsymbol{r})$, which refers to interacting particles and is obtained from eq. [1] with $\hat{A} = \nabla_r \nabla_{r'}$:

$$D = \frac{1}{2}G(\boldsymbol{r}) - \frac{1}{8}\frac{|\nabla\rho(\boldsymbol{r})|^2}{\rho(\boldsymbol{r})}$$

D_σ derived accordingly is no longer the local excess of kinetic energy due to the Pauli repulsion but has the meaning of a local excess of kinetic energy due to both Fermi and Coulomb holes. Its physical signification is less clear because eq. [1] is not formally equal to the Laplacian of the single determinental conditional probability. This definition might be, however, useful in actual calculations where correlated wavefunctions and natural orbitals are available instead of Kohn–Sham orbitals.

[3] A gradient dynamical system is a vector field that is defined as the gradient field of a given function called the potential function. By analogy with a velocity field, one can build trajectories that form the phase portrait of the dynamical system. Of particular importance are the sets of points where the gradient vanishes. These critical points are either local minima (repellors), saddle points, or local maxima (attractors) of the potential function. The basin of an attractor is the set of points lying on the trajectories ending in the neighbourhood of this attractor. Basins are separated by manifolds called separatrices.

[4] In topology, a domain is defined as a set of points that satisfies the following property: for any pair of points a and b belonging to the domain, there exists at least a path joining a and b and totally contained in the domain.

Table 1. Nomenclature of valence attractors.

Synaptic order	Nomenclature	Symbol
0	Asynaptic	V
1	Monosynaptic	$V(X_i)$
2	Disnaptic	$V(X_i, Y_j)$
≥3	Polysynaptic	$V(X_i, Y_j, ...)$

the number of cores connected to a valence basin. The ELF maps of Li_2 and LiH are represented in a plane containing the internuclear axis. We expect a valence basin containing the proton and a core basin in LiH, a valence basin and two core basins in Li_2. In LiH, there are two ~0.5 localization domains that are bounded by the brick-red lines: the first one is an elongated disk that is contained in the lithium core basin; the second, corresponding to the space remaining outside of the blue zones of low ELF, is in the valence basin. The separatrix between the two basins lies within the blue ring. For Li_2, there are three such ~0.5 localization domains. In Li_2, any core basin is connected to the valence basin because (*i*) they share a common separatrix and (*ii*) the 10^{-3} au isodensity contour represented by the broken line is totally contained in the ~0.5 localization domain (and *a fortiori* in the 0.3 domain). We should say that the valence attractor (located at the midpoint of the internuclear distance) is connected to the two lithium cores. On the contrary, for LiH, though condition (*i*) is fulfilled, condition (*ii*) is not because the broken line crosses the blue and green zones and, therefore, the separatrix. Inside the 10^{-3} au isodensity, the *f*-bounding isosurface does not close up the core for any value of ELF above the valence-core merging and, thus, the valence protonated attractor is not connected to the lithium core.

The number of cores connected to a given valence attractor determines its synaptic order. To avoid misleading confusion between valence attractors and orbital vocabulary we have been moved to introduce a new nomenclature of valence attractors, which is given in Table 1. Hydrogen is a particular case because it is, with helium, the only coreless atom. Therefore, as in Lewis theory, it has to be considered as an exception. Hydrogenated attractors are intermediate between core and valence attractors. In our description of the chemical bond, an attractor whose basin contains a proton is considered as a valence attractor and will be designated as protonated; to establish its synaptic order the proton is counted as a formal core basin (for example: a C—H bond is characterized by an protonated disynaptic attractor). In the examples represented in Fig. 1 (see Plate 1), the Li_2 valence attractor is disynaptic whereas the LiH valence attractor is protonated and monosynaptic.

In the present paper, the attractors and their basins will be labeled as $T_{[i]}$(atom labels). T denotes the type of attractor, V for valence, C for core; *i* is an optional running number in the case of multiple attractors related to the same atom(s). For example, in the water molecule there is one core attractor for the oxygen *K*-shell labeled C(O), two protonated disynaptic attractors $V(H_1, O)$ and $V(H_2, O)$, and two monosynaptic attractors corresponding to the lone pairs $V_1(O)$ and $V_2(O)$. In ethane, the disynaptic attractor of the C—C bond will accordingly be named $V(C_1, C_2)$.

The classification of bonds previously proposed remains valid with this new nomenclature. The shared electron interaction is characterized by a di- or polysynaptic attractor. The lone pairs of electronegative atoms are monosynaptic attractors.

2.3. Localization basin integrated density and related properties

The partition of the molecular space into basins of attractors allows the calculation of related properties by integration of the densities of property over the basins (20). In particular, for a basin labeled Ω_A, one can define the average population as :

$$[7] \quad \bar{N}(\Omega_A) = \int_{\Omega_A} \rho(\boldsymbol{r})\, d\boldsymbol{r}$$

Within the framework of our theory, these average populations are referred to as core, bond, and nonbonding (i.e., lone pair) populations according to the type of attractor that defines the basin. Such average populations over ELF basins were first calculated by us (21, 22) and recently by Häussermann et al. for intermetallic solids (23). They are not expected to have integral values and the bond populations would be about twice the topologically defined bond orders (7, 8).

The RMS deviation $\sigma(\bar{N};\Omega_A))$ is defined by (24, 25):

$$[8] \quad \sigma^2(\bar{N};\Omega_A)) = \langle N^2\rangle_{\Omega_A} - \langle N\rangle^2_{\Omega_A}$$

It represents the quantum mechanical uncertainty on $\bar{N}(\Omega_A)$. The variance (or fluctuation) σ^2 was investigated by Bader in the framework of atomic basins (26). The variance is expressed in terms of the diagonal elements of the first ($\rho(\boldsymbol{x})$) and second-order ($\pi(\boldsymbol{x}_1,\boldsymbol{x}_2)$) density matrices (11) as:

$$[9] \quad \sigma^2(\bar{N};\Omega) = \int_\Omega d\boldsymbol{x}_1 \int_\Omega d\boldsymbol{x}_2 \pi(\boldsymbol{x}_1,\boldsymbol{x}_2) + \bar{N}(\Omega) - \left[\bar{N}(\Omega)\right]^2$$

in which $\boldsymbol{x}_i$ denotes the space and spin coordinates of the electron labeled *i*. For a single determinental wave function (i.e., Hartree–Fock or Kohn–Sham) $\sigma^2(\bar{N};\Omega)$ is the difference between the basin population and the integral over the basin of the exchange part of the second-order density matrix:

$$[10] \quad \sigma^2(\bar{N};\Omega) = \bar{N}(\Omega) - B(\Omega,\Omega)$$

In terms of the orbitals $\phi_i(\boldsymbol{r})$ and of the occupations n_i^α, n_i^β, $B(\Omega,\Omega)$ is given by:

$$[11] \quad B(\Omega,\Omega) = \sum_i \sum_j (n_i^\alpha n_j^\alpha + n_i^\beta n_j^\beta)\langle\phi_i|\phi_j\rangle_\Omega\langle\phi_j|\phi_i\rangle_\Omega$$

in which

$$[12] \quad \langle\phi_i|\phi_j\rangle_\Omega = \int_\Omega d\boldsymbol{r}\phi_i^*(\boldsymbol{r})\phi_j(\boldsymbol{r})$$

It is also convenient to define the interbasin integrated exchange density:

$$[13] \quad B(\Omega_A,\Omega_B) = \sum_i \sum_j (n_i^\alpha n_j^\alpha + n_i^\beta n_j^\beta)\langle\phi_i|\phi_j\rangle_{\Omega_A}\langle\phi_j|\phi_i\rangle_{\Omega_B}$$

The fluctuation in a superbasin $\Omega_A \cup \Omega_B$ is:

$$[14] \quad \sigma^2(\bar{N};\Omega_A \cup \Omega_B) = \sigma^2(\bar{N};\Omega_A) + \sigma^2(\bar{N};\Omega_B) - 2B(\Omega_A,\Omega_B)$$

and for the whole space

$$[15] \quad \sigma^2(\bar{N};\Omega_A \cup \Omega_B \cup \ldots) = 0$$

It follows from eq. [14] that for independent basins σ^2 is an extensive quantity. Following Bader (26), it is useful to introduce the relative fluctuation

$$[16] \quad \lambda(\Omega) = \sigma^2(\bar{N};\Omega)/\bar{N}(\Omega)$$

which is positive and also expected to be less than 1.

Another criterion of discrimination between basins is provided by the reduction of reducible domains. The reduction of a reducible localization domain occurs at a critical value of the bounding isosurface, over which the domain is split into domains containing fewer attractors. The localization domains are then ordered with respect to the ELF critical values, yielding bifurcations. Starting at a very low ELF value, we find only one localization domain (the whole space for $\eta(\boldsymbol{r}) = 0$) upon increase of the isosurface defining value, we meet a first separation between valence and core domains, and at higher ELF values the valence reducible domain is split in its turn. The hierarchy of the bifurcation can be visualized by a tree-diagram.

3. Results and discussion

The calculations were performed at the DFT level with Gaussian94 software (27). The standard 6-31G** basis set (28) was used in conjunction with Becke exchange (29) and Lee, Yang, and Parr correlation (30) functionals. All structures were fully optimized. The labeling of atoms that will be used to label the attractors of the ELF vector gradient field is given in Fig. 4.

Figure 2 (see Plate 1) displays the $\eta(\boldsymbol{r}) = 0.8$ localization domains of ethylene, allyl cation, and *trans*-butadiene whereas the $\eta(\boldsymbol{r}) = 0.5$ and $\eta(\boldsymbol{r}) = 0.8$ localization domains of benzene are represented in Fig. 3 (Plate 1). The representation provided by the topological analysis of ELF does not correspond to the conventional picture of a double bond made into σ and π bonds. This latter description is not invariant upon a unitary transformation of the molecular orbitals; alternative representations such as "banana double bonds" have been shown to be equivalent (3).

3.1. Ethylene

In ethylene there are two core attractors, labeled $C(C_1)$ and $C(C_2)$, four protonated disynaptic attractors, $V(C_i, H_j)$, and two disynaptic attractors $V_1(C_1, C_2)$ and $V_2(C_1, C_2)$. The attractor basins that surround $C(C_1)$ are $V(C_1, H_1)$, $V(C_1, H_2)$, $V_1(C_1, C_2)$, and $V_2(C_1, C_2)$ whereas around $C(C_2)$ we find $V(C_2, H_3)$, $V(C_2, H_4)$, $V_1(C_1, C_2)$, and $V_2(C_1, C_2)$. Therefore, the $V(C_i, H_j)$ and the $V_i(C_1, C_2)$ are disynaptic, according to the definition given in a previous section. The basin populations, their standard deviation and relative fluctuations are listed in Table 2. The basins of the two disynaptic attractors have been gathered together in the superbasin labeled $V_{1\cup2}(C_1C_2)$. The basin population corresponding to

Fig. 4. Atomic labels of ethylene, propene, allyl cation, *trans*-butadiene, and benzene.

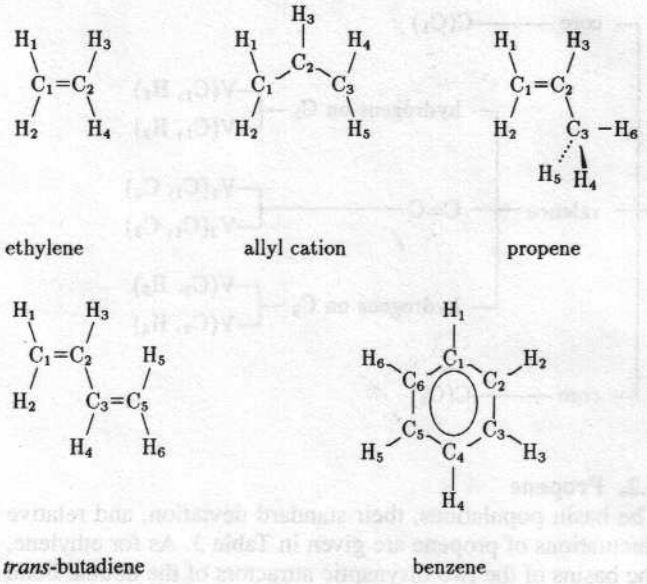

Table 2. ELF value at attractor, basin population, standard deviation, and relative fluctuations of the basin populations of ethylene.

	ELF	$\bar{N}$	$\sigma(\bar{N};\Omega)$	$\lambda(\Omega)$
C(C)	1.0	2.09	0.51	0.12
$V(C_1, H_1)$	1.0	2.04	0.94	0.43
$V(C_1, C_2)$	0.93	1.81	1.12	0.70
$V_{1\cup2}(C_1, C_2)$	0.93	3.62	1.47	0.40

the C=C double bond is less then 4, whereas the core and hydrogen basins are slightly greater than 2. The topological bond orders of Cioslowski and Mixon (7) and of Angyán et al. (8) calculated with the same carbon basis set at the SCF level are, respectively, 1.958 and 1.984. With a 6-31++G** basis these values are reduced to 1.881 and 1.918 whereas the C—H bond order is increased by 0.012 e^-. The discrepancy with our value (1.79) is due in part to different definitions and also to the fact that in our calculation the core population is independently treated. The relative fluctuation in the population of the core basins is low. On the contrary, for basins of the disynaptic attractors of the C=C bond the relative fluctuation is very high (0.7). These two basins are strongly correlated and their aggregation lowers the relative fluctuation from 0.70 to 0.40.

The bifurcation graph (Fig. 5) provides a hierarchy that is consistent with the relative fluctuation values. At $\eta(\boldsymbol{r}) = 0.06$, there is a first partition into core and valence basins. The valence basin is split into two protonated reducible domains $V(C_1, H_1) \cup V(C_1, H_2)$, $V(C_2, H_3) \cup V(C_2, H_4)$, and the $V_{1\cup2}(C_1, C_2)$ one $V_1(C_1, C_2) \cup V_2(C_1, C_2)$ at $\eta(\boldsymbol{r}) = 0.64$. This bifurcation is immediately followed at $\eta(\boldsymbol{r}) = 0.65$ by the reduction of the two protonated domains. Finally, $V_{1\cup2}(C_1, C_2)$ is reduced at $\eta(\boldsymbol{r}) = 0.92$, a value very close to that of the attractors.

Fig. 5. Localization domain reduction tree-diagram of ethylene.

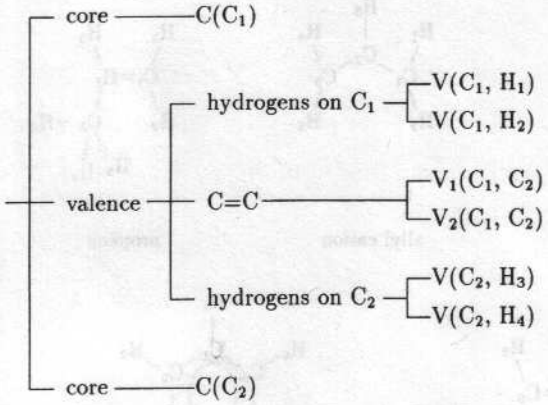

3.2. Propene

The basin populations, their standard deviation, and relative fluctuations of propene are given in Table 3. As for ethylene, the basins of the two disynaptic attractors of the double bond have been merged. The $V_{1\cup2}(C_1, C_2)$ population is larger in propene than in ethylene by 0.1 e^-. The relative fluctuation for this basin, 0.41, is very close to the corresponding value in ethylene. The same value is also found for the $V(C_2, C_3)$ basin, which corresponds to the single C—C bond. The lowering of the molecular symmetry from D_{4h} in ethylene to C_s in propene weakens the correlation between the allylic hydrogen basins; their relative fluctuations decrease by about 0.1. An important correlation remains between the two methyl hydrogens symmetric with respect to the σ plane.

The bifurcation graph of the localization domains of propene is shown in Fig. 6. After the core–valence separation at $\eta(\boldsymbol{r}) = 0.06$, the valence domain undergoes a second separation into three domains at $\eta(\boldsymbol{r}) = 0.65$. These domains correspond to the central carbon hydrogen, the methyl group, and the allyl group. The methyl group domain is reduced at $\eta(\boldsymbol{r}) = 0.67$ into two components $V(C_2, C_3)$ and the domain of the three hydrogens from which the in-plane hydrogen is separated at $\eta(\boldsymbol{r}) = 0.69$, the two out-of-plane being ultimately split for $\eta(\boldsymbol{r}) = 0.70$. On the allyl side, hydrogens detachments occur successively at $\eta(\boldsymbol{r}) = 0.67$ and $\eta(\boldsymbol{r}) = 0.69$ and the reduction of the C═C domain at $\eta(\boldsymbol{r}) = 0.93$.

3.3. Allyl cation

In ethylene and propene the number of attractors is equal to the number of occupied Kohn–Sham orbitals; in allyl cation, there are 10 attractors for 11 doubly occupied orbitals. One disynaptic attractor with a basin population of 2.6 (Table 4) is found for each C—C bond. The value of ELF at the attractor is slightly less than that of the propene single bond. The relative fluctuation for the basins of these attractors, 0.55, is higher than for a double or a single C—C bond in the absence of conjugation, indicating a noticeable delocalization. Delocalization over hydrogen basins is of the order found in propene since the corresponding relative fluctuations are both of the order of 0.30.

The localization domain reduction pattern (Fig. 7) reflects the symmetry of the system. As in propene, the first splitting of the valence domain at $\eta(\boldsymbol{r}) = 0.59$ is due to the detachment of the central carbon hydrogen. The second valence separation ($\eta(\boldsymbol{r}) = 0.645$) involves hydrogens linked to the terminal carbon, which are immediately ($\eta(\boldsymbol{r}) = 0.65$) followed by domains containing the disynaptic C—C attractors. At ($\eta(\boldsymbol{r}) = 0.66$) the domains are totally reduced. It is worth noting that delocalization delays the separation of the $V(C_1, C_2)$ and $V(C_2, C_3)$ domains with respect to the allyl–methyl separation in propene.

Table 3. ELF value at attractor, basin population, standard deviation, and relative fluctuations of the basin populations of propene.

	ELF	$\bar{N}$	$\sigma(\bar{N}; \Omega)$	$\lambda(\Omega)$
C(C)	1.0	2.09	0.51	0.12
$V(C_1, H_1)$	1.0	2.05	0.79	0.31
(C_3, H_4)	1.0	1.98	0.93	0.44
(C_3, H_6)	1.0	1.99	0.75	0.28
$V_{1\cup2}(C_1, C_2)$	0.93	3.68	1.22	0.41
(C_2, C_3)	0.96	1.91	1.0	0.41

Fig. 6. Localization domain reduction tree-diagram of propene.

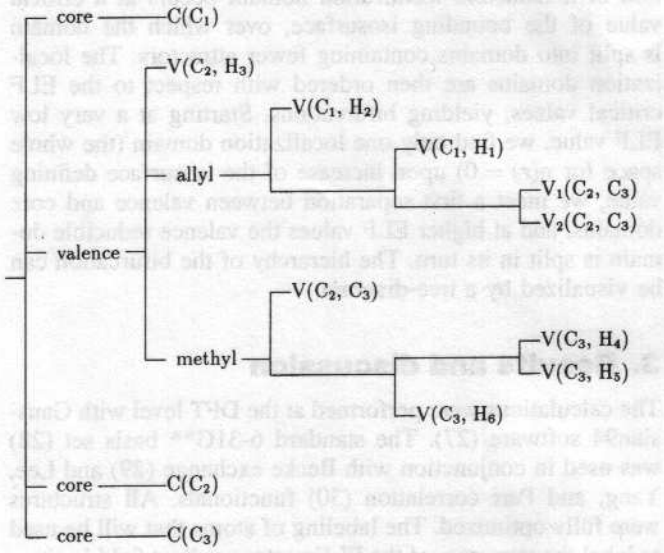

Table 4. ELF value at attractor, basin population, standard deviation, and relative fluctuations of the basin populations of allyl cation.

	ELF	$\bar{N}$	$\sigma(\bar{N}; \Omega)$	$\lambda(\Omega)$
C(C)	1.0	2.09	0.51	0.12
$V(C_1, H_1)$	1.0	2.10	0.78	0.29
$V(C_2, H_3)$	1.0	2.12	0.80	0.30
$V(C_1, C_2)$	0.95	2.60	1.19	0.55

3.4. *trans*-Butadiene

The populations of the attractor basins of *trans*-butadiene, reported in Table 5, show similarities to and differences from

Fig. 7. Localization domain reduction tree-diagram of allyl cation.

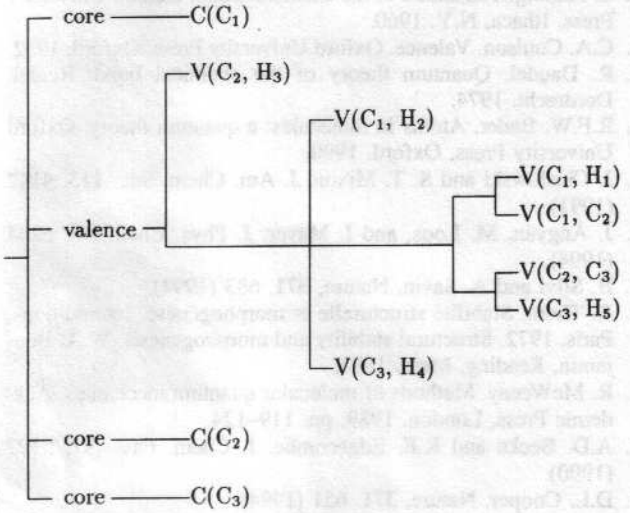

Table 5. ELF value at attractor, basin population, standard deviation, and relative fluctuations of the basin populations of *trans*-butadiene.

	ELF	$\bar{N}$	$\sigma(\bar{N}; \Omega)$	$\lambda(\Omega)$
C(C)	1.0	2.09	0.51	0.12
$V(C_1, H_1)$	1.0	2.05	0.79	0.31
$V(C_2, H_3)$	1.0	2.05	0.79	0.31
$V_{1\cup2}(C_1, C_2)$	0.93	3.56	1.23	0.42
$V(C_2, C_3)$	0.96	2.17	1.04	0.50

Fig. 8. Localization domain reduction tree-diagram of *trans*-butadiene.

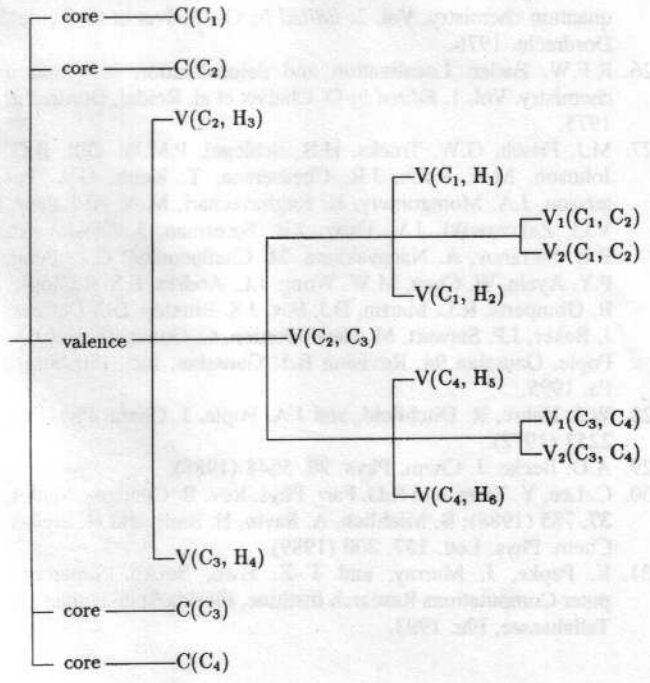

Table 6. ELF value at attractor, basin population, standard deviation, and relative fluctuations of the basin populations of benzene.

	ELF	$\bar{N}$	$\sigma(\bar{N}; \Omega)$	$\lambda(\Omega)$
C(C)	1.0	2.09	0.51	0.12
$V(C_i, C_j)$	0.94	2.83	1.14	0.47
$V(C_i, H_i)$	1.0	2.08	0.80	0.31

that of propene. On the one hand, the ELF values at the attractors are identical in *trans*-butadiene and in propene and the populations of the hydrogen basins are equal to that of the allylic hydrogens; on the other hand, the populations of the double bond attractors are less than that of propene by 1/8 e^-, whereas the single bond basin population is increased by 1/4 e^-. This reorganization of the basin population is an indication of the delocalization along the carbon skeleton. Note also, the increase with respect to propene of the relative fluctuation of the single C—C bond basin.

The localization domain reduction diagram of *trans*-butadiene (Fig. 8) is very similar to that of propene. After the core–valence separation at $\eta(\boldsymbol{r}) = 0.06$, the domains of the protonated disynaptic attractors linked to the carbons of the single bond part from the valence domain at $\eta(\boldsymbol{r}) = 0.63$. The next step, at $\eta(\boldsymbol{r}) = 0.64$, isolates the disynaptic attractor of the C—C single bond from two allylic fragments. At higher ELF values, the two allylic fragments are split in accordance with the way followed in propene, except that the two hydrogen basins are simultaneously detached from the C=C domain.

3.5. Benzene

There are 18 attractors in benzene: 6 core, 6 protonated disynaptic, and 6 C—C disynaptic. Each V(C—C) has a basin population of 2.83 e^-, which compares with the topological bond order, ~ 1.4(7, 8). Delocalization along the skeletal ring is indicated by a rather high relative fluctuation, 0.47 (Table 6). The ELF analysis does not give evidence for any σ and π systems in benzene.

The reduction of the localization domains in benzene, presented in Fig. 9, is very simple and is ruled by the molecular symmetry. At $\eta(\boldsymbol{r}) = 0.06$ the core domains are separated from the valence domain, which undergoes two successive splittings. The first one at $\eta(\boldsymbol{r}) = 0.65$ plucks off the hydrogen, the second, at $\eta(\rho) = 0.68$ unties the $V(C_i, C_j)$ domains.

4. Conclusion

For the electron density produced by a given potential of the nuclei, ELF provides a structuring of the molecular space into basins that may be roughly associated with the electron-pairing regions and have therefore a chemical meaning. The average number of electrons per basin is obtained by integration of the electron density function over the basins. For the systems investigated here, it corresponds roughly to the number of electrons expected on chemical grounds.

Quantum mechanical uncertainty yields standard deviations that typically range from 0.5 for the well-separated

Fig. 9. Localization domain reduction tree-diagram of benzene.

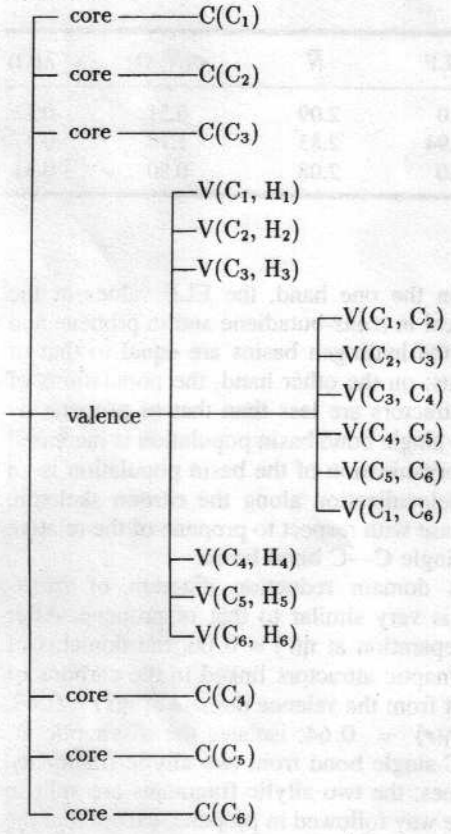

core basins to 1.2 for the valence basins. The core basins are well separated from the valence basins because the value of ELF on the separatrix (i.e., at the border) is always very low, ~0.06. This is not the case between valence basins that are separated at higher ELF values, about 0.6–0.7 for the systems presented here. Following Bader (26), we found that the relative fluctuation is a good measure of the delocalization. It is of the order of 0.1 for core basins, 0.3 for basins of the protonated disynaptic attractor of the C—H bonds, 0.4 for basins related to single and double C—C bonds, and 0.5 for delocalized bonds. Of course, the relative fluctuation is not the only measure of delocalization, which is also reflected by the average basin populations of the C—C bonds (e.g., 2.8 for benzene).

This work illustrates the importance of Richard Bader's contribution to theoretical chemistry. Beyond the theory of Atoms in Molecules, he demonstrated the importance of topological analysis for scrutinizing molecular space and he introduced tools, such as fluctuation analysis, that are very useful complements to the topological approach.

Acknowledgements

The authors gratefully acknowledge M. Kohout's comments on the draft manuscript. The data analyzer software SciAn (31) was used to produce Figs. 2 and 3.

References

1. M.L. Huggins. Science, **55**, 679 (1922).
2. M. Karplus and R.N. Porter. Atoms and molecules. An introduction for students of physical chemistry. W.A. Benjamin, New York. 1970.
3. L. Pauling. The nature of the chemical bond. Cornell University Press, Ithaca, N.Y. 1960.
4. C.A. Coulson. Valence. Oxford University Press, Oxford. 1952.
5. R. Daudel. Quantum theory of the chemical bond. Reidel, Dordrecht. 1974.
6. R.F.W. Bader. Atoms in molecules: a quantum theory. Oxford University Press, Oxford. 1990.
7. J. Cioslowski and S. T. Mixon. J. Am. Chem. Soc. **113**, 4142 (1991).
8. J. Ángyán, M. Loos, and I. Mayer. J. Phys. Chem. **98**, 5244 (1994).
9. B. Silvi and A. Savin. Nature, **371**, 683 (1994).
10. R. Thom. Stabilité structurelle et morphogénèse. Intereditions, Paris. 1972. Structural stability and morphogenesis. W.A. Benjamin, Reading, Mass. 1975.
11. R. McWeeny. Methods of molecular quantum mechanics. Academic Press, London. 1989. pp. 119–124.
12. A.D. Becke and K.E. Edgecombe. J. Chem. Phys. **92**, 5397 (1990).
13. D.L. Cooper. Nature, **371**, 651 (1994).
14. A. Savin, O. Jepsen, J. Flad, O.K. Andersen, H. Preuss, and H.G. von Schnering. Angew. Chem. **31**, 187 (1992).
15. W. Kohn and L.J. Sham. Phys. Rev. [Sect.] A, **140**, 1133 (1965).
16. C.F. von Weizsäcker. Z. Phys. **96**, 431 (1935).
17. Y. Tal and R.F.W. Bader. Int. J. Quantum Chem. **S12**, 153 (1978).
18. P. Mezey. Can. J. Chem. **72**, 928 (1994).
19. R.F.W. Bader, M.T. Carroll, J.R. Cheeseman, and C. Chang. J. Am. Chem. Soc. **109**, 7968 (1987).
20. F.W. Biegler-König, R.F.W. Bader, and T.H. Tang. J. Comput. Chem. **3**, 317 (1982).
21. A. Savin. Second International Conference on Inorganic Chemistry, Sept. 12–15, 1993, Stuttgart, Germany.
22. M. Kohout and A. Savin. Int. J. Quantum Chem. In press.
23. U. Häussermann, S. Wengert, and R. Nesper. Angew. Chem. Int. Ed. Engl. **33**, 2073 (1994).
24. A. Messiah. Mécanique quantique. Tome I. Dunod, Paris. 1962. p. 113.
25. P. Claverie and S. Diner. Localization and delocalization in quantum chemistry. Vol. 2. *Edited by* O. Chalvet et al. Reidel, Dordrecht. 1976.
26. R.F.W. Bader. Localization and delocalization in quantum chemistry. Vol. 1. *Edited by* O. Chalvet et al. Reidel, Dordrecht. 1975.
27. M.J. Frisch, G.W. Trucks, H.B. Schlegel, P.M.W. Gill, B.G. Johnson, M.A. Robb, J.R. Cheeseman, T. Keith, G.A. Petersson, J.A. Montgomery, K. Raghavachari, M.A. Al-Laham, V.G. Zakrzewski, J.V. Ortiz, J.B. Foresman, J. Cioslowski, B.B. Stefanov, A. Nanayakkara, M. Challacombe, C.Y. Peng, P.Y. Ayala, W. Chen, M.W. Wong, J.L. Andres, E.S. Replogle, R. Gomperts, R.L. Martin, D.J. Fox, J.S. Binkley, D.J. Defrees, J. Baker, J.P. Stewart, M. Head-Gordon, C. Gonzalez, and J.A. Pople. Gaussian 94, Revision B.1. Gaussian, Inc., Pittsburgh, Pa. 1995.
28. W.J. Hehre, R. Ditchfield, and J.A. Pople. J. Chem. Phys. **56**, 2257 (1972).
29. A.D. Becke. J. Chem. Phys. **98**, 5648 (1988).
30. C. Lee, Y. Yang, and R.G. Parr. Phys. Rev. B: Condens. Matter, **37**, 785 (1988); B. Miehlich, A. Savin, H. Stoll, and H. Preuss. Chem. Phys. Lett. **157**, 200 (1989).
31. E. Pepke, J. Murray, and T.-Z. Hwu. SciAn. Supercomputer Computations Research Institute, Florida State University, Tallahassee, Fla. 1993.